Supporting Information for "Sensitivity of Tropical Extreme Precipitation to Surface Warming in Aquaplanet Experiments Using a Global Nonhydrostatic Model"

Contents of this file

S1. Derivation of the scaling of sensitivity of tropical extreme precipitation to warming

We start from the definition of liquid ice water static energy (h_L) and total ice water

mixing ratio q_T:

$$h_L = h - L_v q_T, \tag{1}$$

$$q_T = q + q_r + q_c + q_s + q_g + q_i + l, \tag{2}$$

where h is moist static energy, L_v is latent heat of vaporization, q is water vapor mixing ratio, q_r is rain mixing ratio, q_c is cloud water mixing ratio, q_s is snow mixing ratio, q_g graupel mixing ratio, q_i is cloud ice mixing ratio and l is liquid water mixing ratio. We have neglected the differences between latent heat of vaporization and sublimation ($L_v \approx L_S$).

Having $h = s + L_v q$, where s is dry static energy, and replacing equation 2 in equation 1 we have:

$$h_L = s - L_v(q_r + q_c + q_s + q_g + q_i) - L_v l. \tag{3}$$

Since h_L is conserved in adiabatic fluid parcel displacements:

$$\left[\frac{Dh_L}{Dt}\right] = \left[\frac{Ds}{Dt}\right] - L_v \left[\frac{D(q_r + q_c + q_s + q_g + q_i)}{Dt}\right] - L_v P = 0, \tag{4}$$

where $P = Dl/Dt$ is surface precipitation and the square brackets denote vertical integration:

$$[\cdots] = -\int_{surface}^{100hPa} (\cdots)\frac{dp}{g}. \tag{5}$$

Thus:

$$\left[\frac{Ds}{Dt}\right] = L_v \left[\frac{D(q_r + q_c + q_s + q_g + q_i)}{Dt}\right] + L_v P. \tag{6}$$

The left side of equation 6 can be written as:

$$\left[\frac{Ds}{Dt}\right] = \left[\frac{\partial s}{\partial t}\right] + \left[u\frac{\partial s}{\partial x}\right] + \left[v\frac{\partial s}{\partial y}\right] + \left[-\omega\frac{\partial s}{\partial p}\right], \tag{7}$$

where u, v and ω are zonal wind, meridional wind and pressure velocity, respectively. When extreme precipitation occurs, vertical advection (last term on the right side of equation 7) is the main contributor to the budget for all resolutions with explicit convection and for R2B4 and R2B5 with parametrized convection (Figure S2). In those resolutions, we can approximate the tendency equation of dry static energy by the vertical advection term:

$$\left[\frac{Ds}{Dt}\right] \approx -\left[\omega \frac{\partial s}{\partial p}\right]. \tag{8}$$

On the other hand, when extremes occur, specific humidity approximates the saturation specific humidity for all explicit convection simulations and for R2B4 with parametrized convection. (For the rest of the resolutions with parametrized convection, the atmospheric lapse rate is not restored to its equilibrium state). At those resolutions where this assumption is met, and given the conservation of moist static energy we can write:

$$ds \approx -L_v dq_s. \tag{9}$$

Using this assumption we tracked if the vertically integrated advection of dry static energy is approximated by minus latent heat times the vertical integrated advection saturation specific humidity (equation 10). Figure S4 shows the confirmation of this assumption.

$$\left[\omega \frac{ds}{dp}\right] \approx -L_v \left[\omega \frac{dq_s}{dp}\right]. \tag{10}$$

Introducing equation 10 in equation 8 and using equation 6 to solve for $EP(i)$ (we substitute P by $EP(i)$ since the assumptions are met just for extreme precipitation values), we have:

$$EP(i) \approx \left[w \frac{\partial q_s}{\partial p}\right] - \left[\frac{D(q_r + q_c + q_s + q_g + q_i)}{Dt}\right] \tag{11}$$

Now, we define a precipitation efficiency:

$$\epsilon = 1 - \frac{\left[\frac{D(q_r+q_c+q_s+q_g+q_i)}{Dt}\right]}{\left[w\frac{\partial q_s}{\partial p}\right]}. \tag{12}$$

Finally we get the scaling as the product of precipitation efficiency ϵ and total condensation:

$$EP(i) \approx \epsilon \left[w\frac{\partial q_s}{\partial p}\right]. \tag{13}$$

We test the scaling (equation 13) by computing correlations between the total condensation term and the actual extreme precipitation in our CTL and 4K simulations (Figure S5). As expected from the above assumptions we found that the scaling reproduces the behaviour of extreme precipitation for all resolutions with explicit convection and for R2B4 with parametrized convection.

Using this EP scaling and neglecting changes in precipitation efficiency a SEP can be derived in terms of changes in dynamics and thermodynamics through omega and vertical gradient of saturation specific humidity, respectively.

$$SEP(i) = \frac{\delta EP(i)}{\delta T \cdot EP(i)} \approx \underbrace{\frac{\left[\delta(\omega)\frac{\partial q_s}{\partial p}\right]}{\delta T \cdot \left[\omega\frac{\partial q_s}{\partial p}\right]}}_{Dynamic} + \underbrace{\frac{\left[\omega\delta\frac{\partial q_s}{\partial p}\right]}{\delta T \cdot \left[\omega\frac{\partial q_s}{\partial p}\right]}}_{Thermodynamic}. \tag{14}$$

S2. Convective organization metrics.

1. Subsiding fraction prime (SF´): The development of convective aggregation in GCM is closely associated with the tendency of the atmosphere to develop large areas of dry, subsiding air, and the tendency of convection to clump within narrow areas of large-scale ascents. SF´ is designed to measure the degree of convective organization in simulations with background circulation (i.e Hadley circulation) that has to be excluded to more

appropriately measure the behavior of individual cumulus convection. To remove the background circulation, the tropics is divided into squared subdomains of 10° longitude and the mean of omega over each subdomain is computed. Then, SF´ is defined as the fractional coverage of negative ω', where $\omega' = \omega - < \omega >$ at each subdomain.

2. Organization index (Iorg): A simple organization index that permits to classify a field as regular, random or clustered. We use a threshold of omega higher or equal to the mean subsiding omega at the level of 500 hPa to distinguish convective grid cells. Then, to identify convective grid cells that are part of the same cluster, eight point connectivity is employed in resolutions R2B6 and R2B8.

3. Organization index with zero connectivity (Iorg_{-0}): For low resolutions the minimum distance to cluster by vicinity used by Iorg is too large and the resulting clusters might not represent individual convective systems. To avoid this issue we identify convective grids cell as individual entities using zero connectivity.

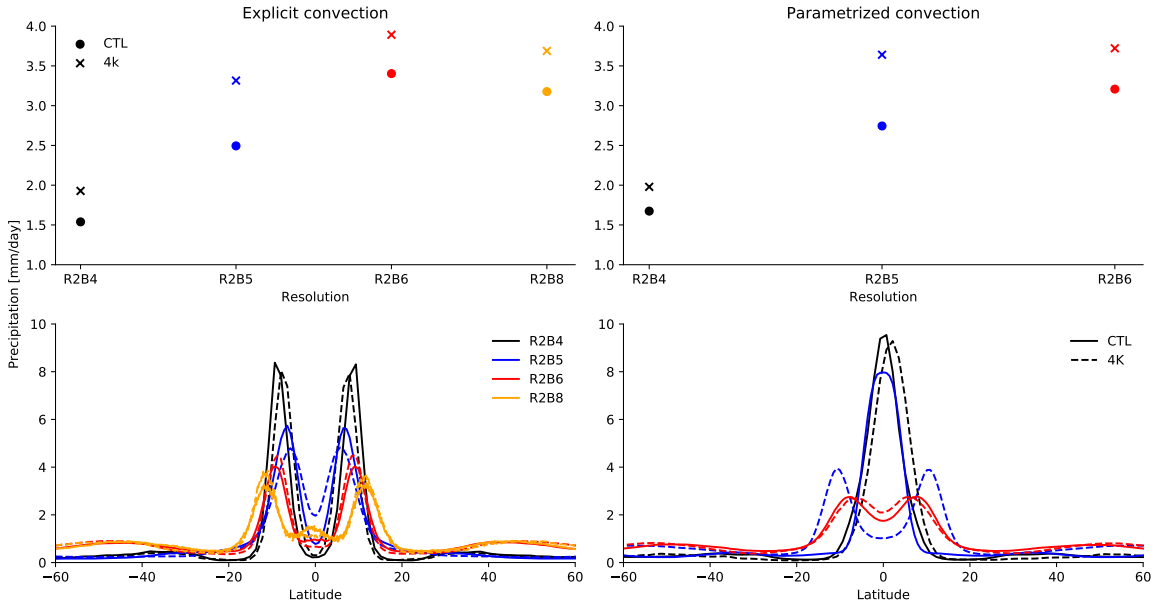

Figure S1. Global mean precipitation (top) and zonal mean precipitation normalized by global mean (bottom). For the comparison, we used a mass-conserving interpolation method to aggregate the results to the coarsest resolution (R2B4) in order to distinguish between the effect of grid size and change in physical processes

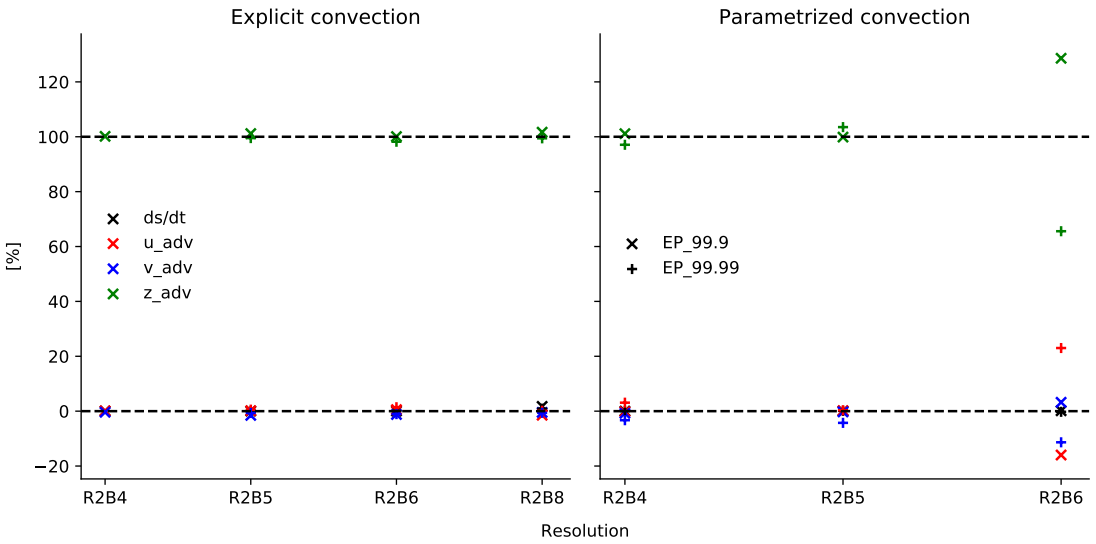

Figure S2. Relative proportion of local change (black), zonal advection (red) meridional advection (blue) and vertical advection (green) of vertical integrated dry static energy to the total vertical integrated material derivative of dry static energy when $EP_{99.9}$ ("x") and $EP_{99.99}$ ("+") occurs.

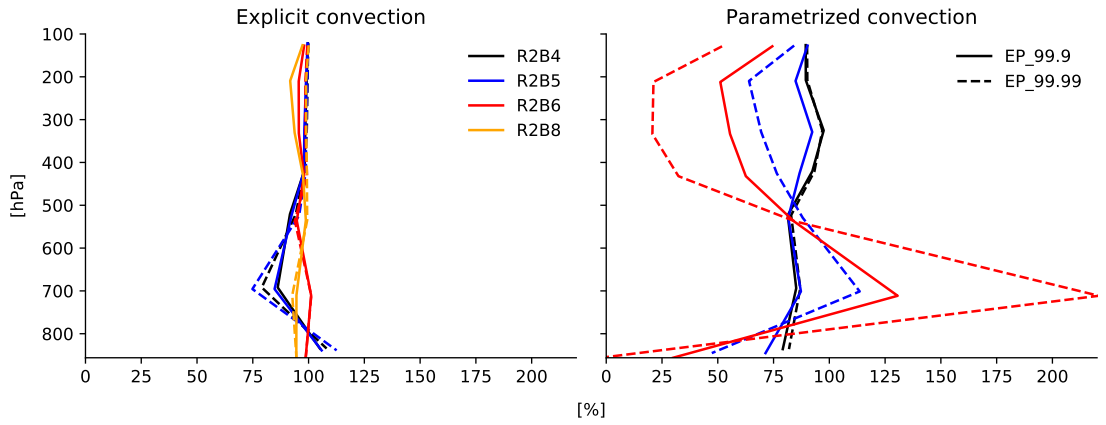

Figure S3. Ratio of specific humidity to saturation specific humidity profiles when $EP_{99.9}$ (solid) and $EP_{99.99}$ (dashed) occurs.

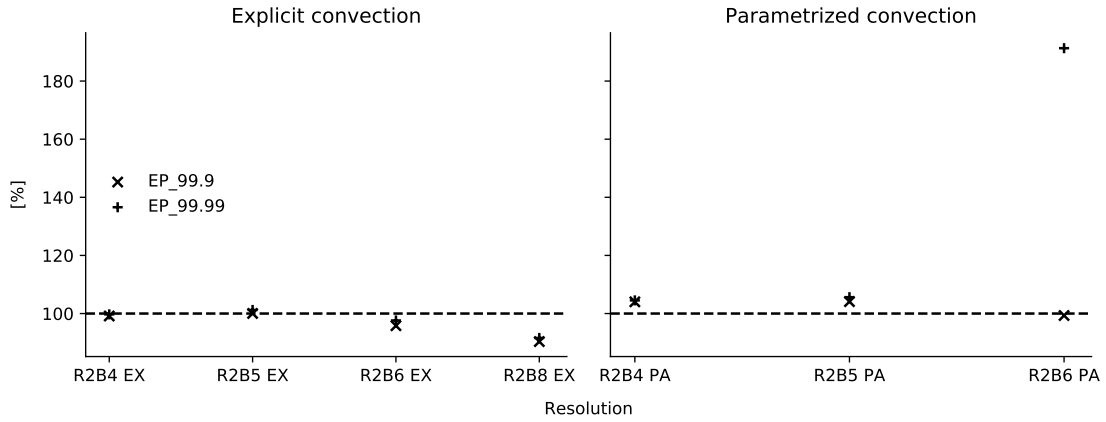

Figure S4. Ratio of negative latent heat times vertical integrated advection of saturation specific humidity to vertical integrated advection of dry static energy when $EP_{99.9}$ ("x") and $EP_{99.99}$ ("+") occurs.

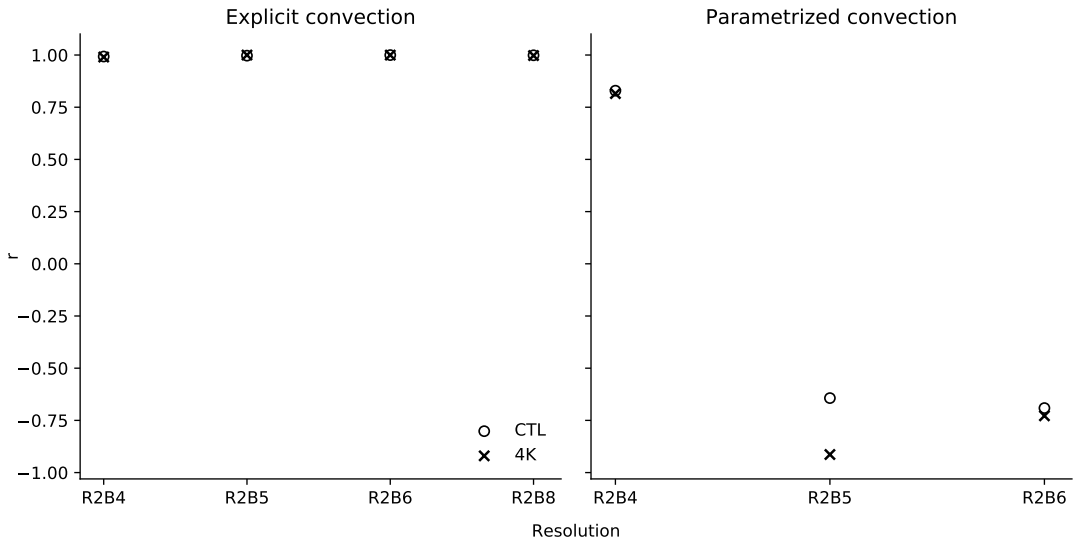

Figure S5. Correlation between total condensation and extreme precipitation.

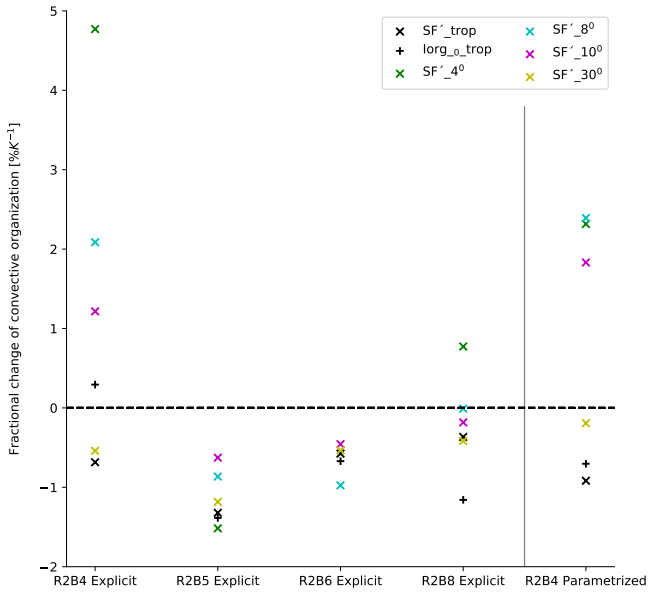

Figure S6. Fractional changes of organization metrics for large scale (SF´_trop and Iorg$_{-0}$_trop) and for subdomains centered where extremes occurs (SF´$_{-30}$, SF´$_{-10}$, SF´$_{-8}$, and SF´$_{-4}$) at coarse grained resolutions to R2B4. Note that, given the resolution of R2B4, a subdomain of 2° x 2° will contain a unique grid point and the fractional change of SF´ will be zero; and subdomains from 6° x 6° and 8° x 8° will contain the same amount of grid points, producing equal fractional changes.